Hindawi
Shock and Vibration
Volume 2021, Article ID 2323758, 16 pages
https://doi.org/10.1155/2021/2323758

Research Article

Effect of the Bracing System on the Probability of Collapse of Steel Structures under Maximum Credible Earthquake

Alireza Kianmehr

Civil and Environmental Engineering, Tarbiat Modares University, Tehran, Iran

Correspondence should be addressed to Alireza Kianmehr; alireza.kianmehr@modares.ac.ir

Received 7 August 2021; Revised 30 August 2021; Accepted 17 September 2021; Published 18 October 2021

Academic Editor: Li Tian

Simple bracing frames can be divided into two types in terms of concentric or eccentric. Concentric bracing frames are frames that intersect with other structural members at one point in the structure along the bracing members. Otherwise, the braced frame will be eccentric. It is said empirically that due to this type of shaping, eccentric bracing frames exhibit more ductile behavior and concentric bracing frames exhibit more stiff behavior. This behavioral difference caused this study to be numerically computing for five frames, including unique concentric and eccentric bracing frames of 5 and 10 stories and an ordinary 5-story concentric bracing frame. Their tensions and drift ratios should be acceptable for the use of residential buildings. Using the primary two steps of the new PEER probabilistic framework, namely, probabilistic seismic hazard analysis and structural analysis, which leads to the drawing of fragility curves, the probability of collapse is obtained to compare the safety capability of these frames according to their different characteristics against earthquakes. The results show that increasing the ductility or increasing the number of floors or the height of these systems can reduce collapse. Also, according to the results of the probability of collapse obtained in frames with 5-story concentric bracing frames, it can be said that some of the current regulations, which work based on previous approaches of analysis, can lead to unsafe structures with a high probability of collapse.

1. Introduction

In the bracing frame, more stability stiffness and uncertainty can be created by connecting the braces to the beams and columns. Moreover, considering the simple connections throughout the frame, the whole structure can be designed more economically. The ductility of such frames is classified into two types, ordinary and special, in Iranian Standard 2800. Ordinary frames cannot be used for structures with a height of more than 15 meters or for sites with very high seismicity and structures with high importance such as hospitals. The types of such frames are shown in Figure 1. In this figure, frame a, diagonal bracing, frames b and c, respectively, inverted V and V bracing, and frame d, x-braced, are cross braces, which have the highest stiffness among all frames, and also frame e shows k-shaped bracing, which from the perspective of the tenth topic of National Building Regulations of Iran is not allowed [1].

In eccentric bracing frames, the extension of the bracing members, unlike the concentric bracing frames, does not meet at one point in the structure and are centered along the column, the middle of the beam, or the end of the other braces in an opening. At the deliberate deviation of the created center, the link beams are placed, depending on their length, shear yield, flexural, or shear-flexural behavior expected with the yield created in this section due to abnormal lateral loads such as. The earthquake does not spread to other structural members and acts as a seismic fuse [3]. Several models of structural arrangement types in eccentric bracing frames are shown in Figure 2. Another difference between the concentric and eccentric bracing systems, as seen in Figure 2, is the presence of transverse stiffeners in the link

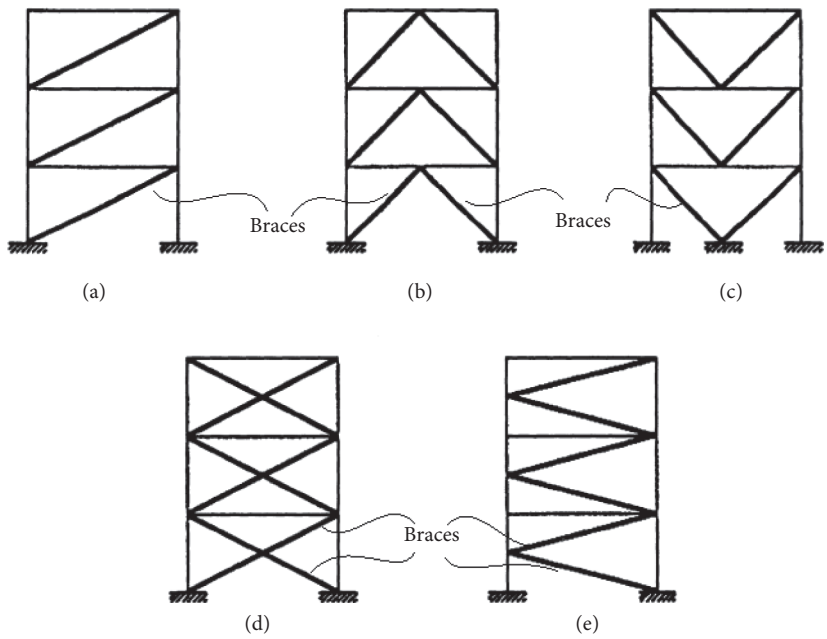

Figure 1: Configuration types of concentric bracing frames [2].

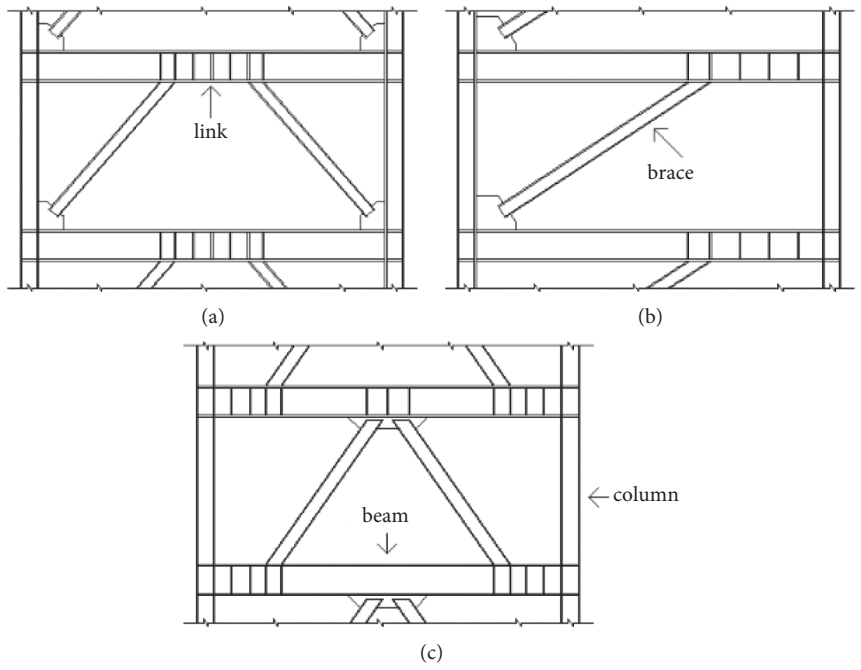

Figure 2: Several schematic models of various structural member arrangement models in frames with eccentric bracing systems [4].

beam due to the shear force and the flexural moment within it due to earthquake forces.

Eccentric bracing frames can exhibit good cyclic behavior and hysteresis if controlled by structural members with high ductility. Iranian Standard 2800 only allows remarkable ductility for such frames and the National Building Regulations No. 10 stated, "The larger the length of the link beam, the less the rotation and deformation." Figure 3 shows the stress expansion in one of the designed connection beams. Significant progress has been made in seismic hazard estimation in recent years. In the framework of the PEER method, the probability of damage to structures due to earthquakes is estimated. In this regard, the Pacific Earthquake Engineering Research Institute is a building risk assessment that is the basis for the next generation of seismic design codes. In this method, the probability of structural failure is determined by the possible combination of hazard and vulnerability functions of structures. The result can be expressed as the probability of various economic losses. In summary, the design approach includes specifying the performance goal (e.g., the

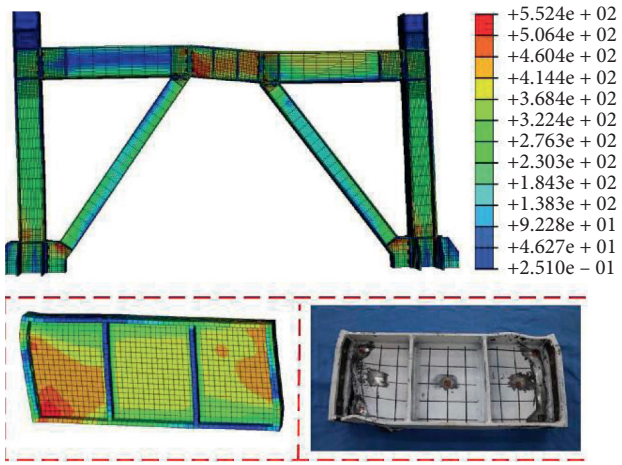

Figure 3: Simulated stress propagation in an eccentric bracing frame and its laboratory sample [6].

acceptable probability of collapse and acceptable financial losses) and associated seismic risk, obtaining engineering parameters to select the system, and finally comparing the performance goal with existing criteria [5].

Figure 4 shows the proposed PBEE framework for design based on probabilistic performance and minimizing the probability of collapse. The framework includes risk analysis, structural analysis, damage analysis, and loss analysis. But if just probability of a collapse needed, the first 2 steps can be the answer. To analyze seismic hazards, the final output is the "IM" parameter or intensity measure, which is taken from hazard curves. Various parameters can be used as intensity measures, such as the maximum ground acceleration in the record (PGA) or spectral acceleration in the first mode (SA (T1)). In the past, when talking about the capacity of the structure, the strength of the structure and related components was associated with the mind, but now the seismic design is based on the emphasis on deformation capacity and energy dissipation. In this regard, the structural response is the engineering demand criterion or EDP, which is generally expressed for a certain level of intensity criterion, and the maximum drift is between classes of its types. In other words, when we talk about the probability of collapse due to maximum ground excitations, we are talking about the probability of reaching the level of various engineering demands (such as drift), which is based on the intensity criteria corresponding to the collapse threshold in the structure. The main relation for the probabilistic expression of the components of PBEE methodology can be expressed by the probability theory of Equation (1), where λ is equal to the rate of occurrence; $G[x \mid y] = P[X > x \mid Y = y]$ means complementary to the cumulative distribution of X under the condition of Y. Data between each stage are distilled into four variables: ground motion Intensity Measure (IM), Engineering Demand Parameter (EDP), Damage Measure (DM), and one or more Decision Variables (DV):

$$\lambda(\mathrm{DV}) = \iiint G<\mathrm{DV} \mid \mathrm{DM}>\mathrm{d}G<\mathrm{DM} \mid \mathrm{EDP}>\mathrm{d}G<\mathrm{EDP} \mid \mathrm{IM}>\mathrm{d}\lambda(\mathrm{IM}). \quad (1)$$

However, if only the first two steps of the PBEE framework in equation (1) are considered, it will take the form of equation (2):

$$\lambda(\mathrm{Collapse}) = \int_{\mathrm{IM}}^{\infty} P\langle \mathrm{Collapse} \mid \mathrm{IM} = \mathrm{im}_i \rangle \mid \mathrm{d}\lambda(\mathrm{IM}). \quad (2)$$

In a study, Yaser Mozaffari and Abbas Akbarpour investigated the estimation of the behavior of structures with eccentric bracing exposed to near-field earthquakes. This study has exposed the same structures to 10 earthquakes, and the focal length of the selected earthquakes is less than 10 km. Based on the performed analyses, they have examined and compared the response of the structures, which is based on the interstory drift and have concluded that in all structures, with each increase in the length of the link beam, these drifts increase. Also, the type of link beam (vertical or horizontal) was considered adequate on the shear base of the studied models [8]. In a study of fragility curves, Bakhshi and Soltanieh developed simple concentric bracing frames for residential use. They reported that a significant number of collapses occur when the braces on the first floor fail and collapse due to the limited possibility of redistribution of forces after that, which was repeated with increasing intensity [9]. Yang et al. investigated the different arrangements of braces (x, v, I, ...). They observed that to satisfy the requirements of CSA S16 in the design of bracing frames and to have an allowable probability of collapse if concentric bracing with X arrangement is used (so that the intersection point of the braces on the bracing beam is one in between), the minimum required steel can be used. This study also concluded that although this arrangement will be the most economical type of bracing arrangement in the structure, it will have a shorter service life [10].

In 2010, Vamvatsikos and Fragiadakis used incremental dynamic analysis to estimate the sensitivity and uncertainty of seismic performance of structures; they found that ductility, negative strength, and negative resistance have high sensitivity in estimating the performance of structures [11]. Lin et al. worked on the effectiveness of braced frames by studying 6 structures with BRB and EBF systems in 6- and 20-story class systems using 20 far and near field records. In this study, they concluded that the effectiveness of the added brace depends on the height and type of ground movements. The bracing frame added in normal ground movements can reduce drift and the possibility of collapse, which is especially true in short-rise buildings. However, in near-field earthquakes, the concentration of failure in the weak floors of the structure increases, and it becomes more difficult to

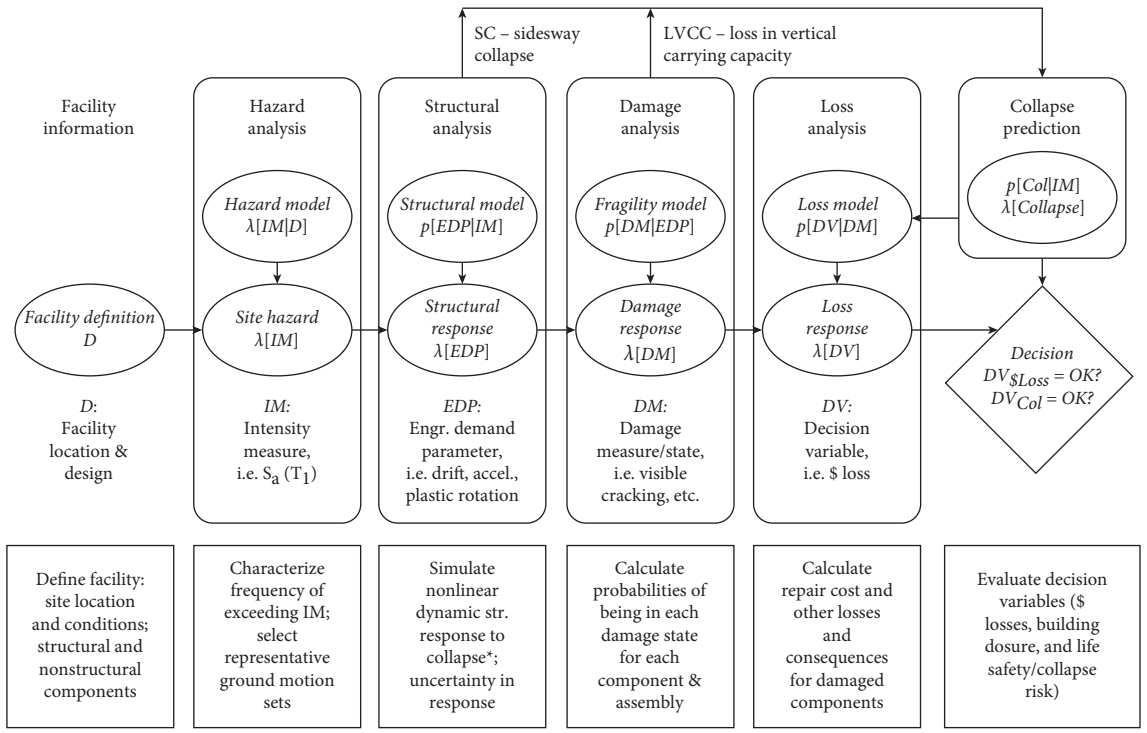

Figure 4: Provided PBEE framework for design based on probabilistic performance and minimizing the probability of collapse [7].

control the failure in the link beam or BRB braces. Therefore, only a limited amount of braced frames added can help resist ground motion near the source [12]. In the present study, to understand the effect of stiffness and ductility, a simple eccentric steel bracing system has been selected as a more ductile system and a simple concentric bracing system as a system with higher stiffness. Performance-based structures tied to the fundamentals of probability science can answer the following questions and discuss the results:

(1) Can simple structural frames that can be designed from the point of view of regulations have an acceptable probability of collapse against maximum ground excitations?

(2) Given the presence of concentric or eccentric bracing systems in simple steel frames, what will be the safety of each of these systems compared with the other?

Using these analytical methods to analyze structures against a phenomenon with completely indeterminate features can inform structural designers about the reliability of the methods of analysis of previous design regulations against earthquakes. Recently, the use of probabilistic analysis methods for the design and analysis of structures has been allowed. The methods used in this research will apply to real projects under design [13].

2. Seismic Parameters and Hazard Analysis

2.1. Engineering Demand Parameter (EDP). In this study, the maximum interstory drift ratio (MIDR) has been selected because the functional level studied was the prevention of the total collapse of the structure. The mentioned criterion has been used in most of the previous researches, and its limits have been mentioned in the newest regulations.

2.2. Seismic Intensity Measure. In selecting the IM seismic intensity measure, three criteria of practicality, efficiency (dispersion), and completeness (adequacy) are essential. One of the desirable properties of a selected IM is less dispersion. The relationship between structural response and seismic intensity measure can be written as equation (3) or (4), where SD is equal to the average response of the structure (DM) under seismic intensity (IM):

$$\mathrm{SD} = a.\mathrm{IM}^{b}, \tag{3}$$

or

$$\ln(\mathrm{SD}) = b.\ \ln(\mathrm{IM}) + \ln(a). \tag{4}$$

The efficiency criterion is measured with the scattering rate in the middle estimation of the results obtained from nonlinear dynamic analysis. An efficient intensity measure reduces the amount of change in the estimated need for an applied intensity measure. Applying an efficient intensity measure reduces the dispersions in the median estimate of the results of nonlinear dynamic analysis. In general, the smaller the scatter of IDA curves with changing seismic acceleration records, the more efficient the IM index used is than the PGA index because Sa(T1) is more efficient. For example, the dispersion of the results is less. Therefore, the

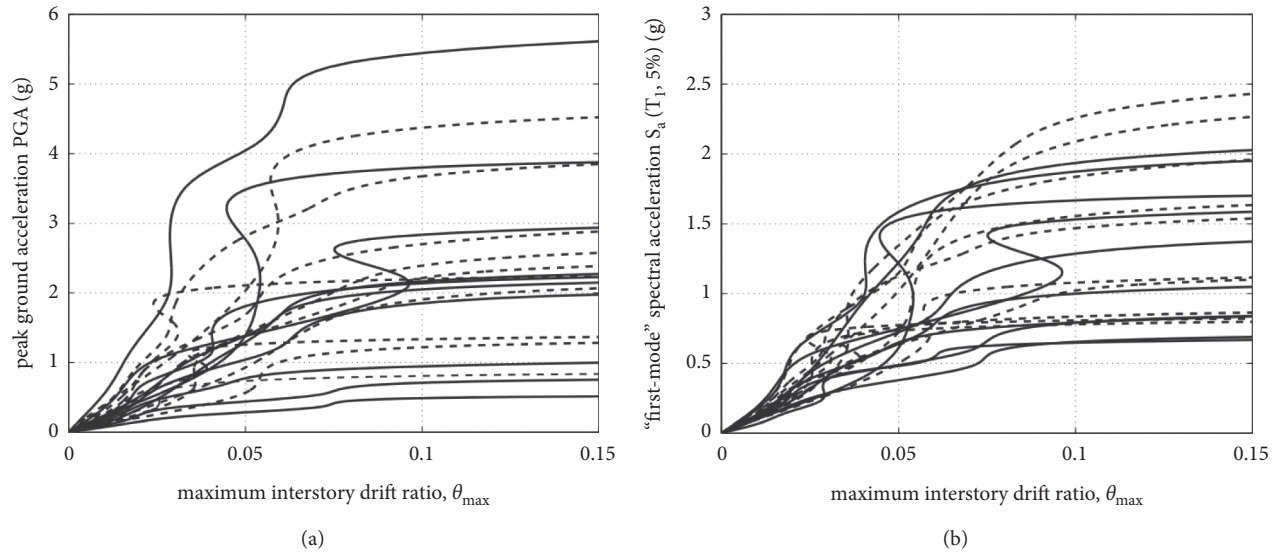

Figure 5: IDA curves for, T1 = 2.2 sec, a 9-story steel moment-resisting frame with fracturing connections plotted against (a) PGA and (b) Sa (T1, 5%) [15].

purpose of efficiency is to reduce changes in IDA curves due to record change.

Figure 5 shows the IDA cure handle of a 9-story steel structure. IDA can be used to determine IM for collapse capacity. In this case, Sa (T1) is better than PGA for this structure because the scatter of IM values with a straight line is less than the previous case (in this figure, the same vertical scales are not considered to see the graphs better, but if the scales are the same, the difference in scattering can be seen better now). Therefore, the seismic intensity parameter according to Shome [14] is spectral acceleration corresponding to the period of the first mode period for damping of 5%, so Sa (T1, 5%) is considered in this study.

2.3. Site Selection, Uniform Hazard Spectrum, and Records. The results of the Iran Seismic Hazard Analysis project, which was carried out by a research team at the University of Tehran, have been placed in the database of the Vice President for Strategic Planning and Supervision as a valid study. In the written report of the project, 3 sites with different soil information and in different parts of Tehran have been selected in terms of seismicity and their uniform hazard spectrum has been obtained [16]; if we want to assume in this study that the models under study are built on type 3 soil, the information obtained according to what was selected for site 2 in the project and with the specifications of Table 1 can be used for the next steps of probabilistic analysis. Uniform hazard spectra of 2475 and 475 years are obtained from the mentioned hazard curves (Figure 6), and the uniform hazard spectrum of 2475 years is used for the following stages of research.

2.4. Selection Ground Motion Records. Because we intend to obtain the structural response using incremental dynamic analysis, the first step in the process of evaluating the

Table 1: Coordinates and soil type of the selected site.

Site	Coordinates	Soil type (2800)	Soil type (NEHRP)
2	(51.42E, 35.64N)	III	D

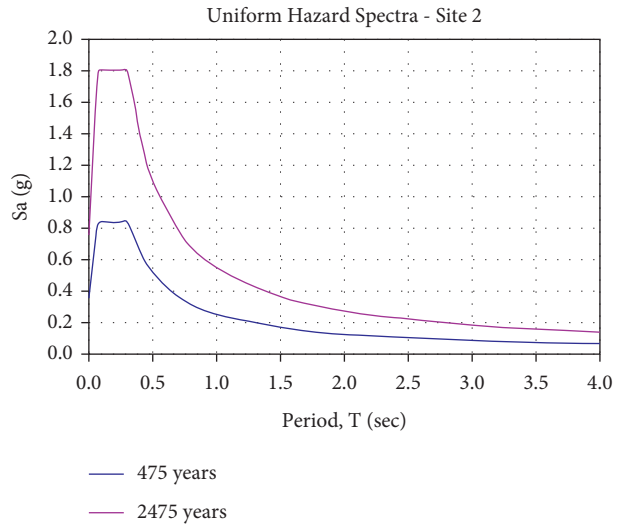

Figure 6: Uniform hazard spectrum of 475 and 2475 years of site no. 2 [16].

performance of drawing IDA curves is to prepare a set of seismic accelerometers so that this set indicates the seismicity of the area. Therefore, in the first step, ground motion records should be selected by almost similar conditions of the region in terms of fault mechanism, distance to the desired site, and the magnitude of the earthquake [17]. The FEMA-P695 guideline for seismic design of structures introduces two categories of near-field and far-field records, which are suitable for seismic design of structures against

MCE earthquakes regardless of the scale factor. To meet the site requirements of the structures in question in the records [18], only records have been selected that had geotechnical conditions of the seismic station with site conditions such as average shear wave velocity up to 30 m depth (V_{S30}) by soil classification of Type 3 from the point view of Standard 2800. It should be noted that this standard specifies the desired speed range of 175 to 375 meters per second. According to the consideration of these conditions, a total of 16 records of far-field and 4 records of near-field without impact have been selected for nonlinear analysis (Table 2) according to the recommendation of Shome [14]. Also, to compare the difference in spectral accelerations associated with each record in each of the frames under study (due to the difference between the main period in each frame compared with the other frame), the spectral acceleration of each frame for its main period is obtained according to the equivalent seismic acceleration spectrum of each record (Table 3).

3. Modeling Frames

3.1. Generalities of Modeling Discussion. The mentioned models have a height of 3 meters on all floors, and also, according to Figure 7 the plan of structures has 6 bays in the X direction and 5 bays in the Y direction. Also, the footing of the columns is articulated, and the interaction of soil and structure has been avoided. It is assumed that each of the studied frames is a two-dimensional frame on the right side of the frames in the Y direction among the frames in the three-dimensional model of the mentioned structure (the frame in the direction of righter north-south axis in the plan of Figure 7). After designing the structural members of the 3D model according to what you will see below, the 2D frame designed while preserving the effects of the 3D structure has been used for incremental dynamic analysis. Also, the loading of structures according to the sixth article of National Regulations of Iran for dead and live load is considered to be 500 and 200 kg/m^2, respectively, which are connected linearly on the beams in proportion to their load-bearing surface; that is, 3.6 meters from the length of the load-bearing floor is distributed. In these frames, there are no irregularities in the 3D model, including irregularities in the distribution of stiffness.

According to the subject of the present study, the composite slab is one of the most widely used types of roofs in steel structures choose, which transfers its load one-way due to the placement of secondary beams. The secondary beams are of IPE160 type and are located at a distance of 50 cm from each other. Also, the thickness of the slab is considered to be 12 cm according to Article 9 of the National Building Regulations of Iran. Also, for reinforcement of slabs in both directions, rebar number 12 (diameter = 12 mm) with $Fy = 400$ MPa is distributed every 15 cm.

For easier reference to each of the systems, the XXX-X naming format is used, the first 3 letters stand for the type of structural system and the last letter indicates the number of floors. Table 4 lists the modeled frames and the abbreviation for each. Modeling of frames in OpenSees uses the concentrated plasticity approach with zero-length rotational springs at the end of each member. The middle elastic member "modelasticbem2d" with "bill material" modifies the stiffness matrix. Uniformity is achieved by changing the maximum resistance and the load resistance to the curve with dynamic cyclic loading such as an earthquake. The damping of the frames is calculated by assuming its uniform distribution in the whole frame by the Rayleigh method and assuming the damping ratio of 5% [19]. Because in this method the damping of the frame is a ratio of the stiffness and mass of the structure, it should be known that the mass of the structure is placed directly on the end nodes. The effect of P-Δ on modeling through supported columns has been considered according to the research of Krawinkler et al. [20]. The specifications of steel materials related to beams, columns, and braces also reinforced concrete used materials related to slabs are also mentioned in Table 5.

3.2. Concentric Bracing Frames. According to the tenth article of the Iran National Building Regulations in this type of lateral bearing system, the models are designed in two categories of ordinary and extraordinary ductility. In ordinary ductility, the bracing members are designed for tensile force only and with a slimming coefficient λ_{md}. So even if the braces cannot experience nonlinear behavior before buckling due to lateral load, their design is acceptable. However, in the remarkable ductility, none of the mentioned facilitators is used. The braces' compression ratio is more diminutive than λ_{hd}. Standard 2800 introduces 15 meters of the maximum allowable height due to these differences in the design of a structure frame with an ordinary concentric bracing frame. Accordingly, the ordinary concentric bracing model is made only for a 5-story frame. It is noteworthy that the structure for the study of this research will be a 2-dimensional frame taken from one of the 3D structure frames. The braces of this group of models are cross-shaped, and their arrangement in the selected plan and frame is presented in Figures 8 and 9. The sections obtained in the design by the criteria of Article 10 of the National Building Regulations of Iran and Standard 2800 for different members of concentric frames are listed in Table 6, and an example of each type of sections used is shown schematically in Figure 10.

For modeling in OpenSees software and performance analysis of frames, the buckling of compression members is proposed. In this regard, the local buckling of the members will not be a control due to the selection of all structural sections of the seismically compacted rolled type, and the global buckling of these members can be controversial. To accentuate the hysterical behavior of the frame, the rotational springs capture hysteretic flexural behavior, including deterioration through the modified Ibarra-Medina-Krawinkler (IMK) model. This modeling approach for columns can capture story mechanisms [21, 22].

In terms of the buckling behavior of braces, according to the recommendation of Urim and Mahin [23], each brace is divided into ten smaller "nonlinear fiber elements." It is made of braces and with corotational geometric

Table 2: Selected records for incremental dynamic analysis.

No.	Earthquake		Station data				
	Name	Station	Magnitude	VS_30 (m/s)	PGA (g)	Site-source distance	Field distance
1	Northridge	Beverly Hills	6.7	356	0.52	17.2	Far field
2	Northridge	Canyon country-WLC	6.7	309	0.48	12.4	Far field
3	Duzce	Turkey Bolu	7.1	326	0.82	12	Far field
4	Imperial Valley	Bonds	6.5	223	0.76	2.7	Near field
5	Imperial Valley	Delta	6.5	275	0.35	22	Far field
6	Imperial Valley	El Centro	6.5	196	0.38	12.5	Far field
7	Imperial Valley	Chihuahua	6.5	275	0.28	7.3	Near field
8	Kobe	Shin-Osaka	6.9	256	0.24	19.2	Far field
9	Kocaeli	Duzce	7.5	276	0.36	15.4	Far field
10	Northridge	Saticoy	6.7	281	0.42	12.1	Near field
11	Landers	Yermo Fire	7.3	354	0.24	23.6	Far field
12	Landers	Coolwater SCE	7.3	271	0.42	19.7	Far field
13	Loma Prieta	Capitola	6.9	289	0.53	15.2	Far field
14	Loma Prieta	Gilroy	6.9	350	0.56	12.8	Far field
15	Kocaeli, Turkey	Yarimca	7.5	297	0.31	4.8	Near field
16	Superstition Hills	El Centro	6.5	192	0.36	18.2	Far field
17	Superstition Hills	Poe Road	6.5	208	0.45	11.2	Far field
18	Cape Mendocino	Rio	7	312	0.55	14.3	Far field
19	Chi-Chi	CHY101	7.6	259	0.44	10	Far field
20	San Fernando	Hollywood Stor	6.6	316	0.21	22.8	Far field

Table 3: Spectral acceleration per response spectrum equivalent to each seismic record.

	Time periods (s)				
	OBF-5	SBF-5	SBF-10	EBF-5	EBF-10
Record no.	0.65	0.58	0.85	0.8	1.18
	Spectral accelerations per record (~g)				
	OBF-5	SBF-5	SBF-10	EBF-5	EBF-10
1	1.179	1.024	0.900	0.934	0.580
2	1.214	1.287	1.079	1.015	0.263
3	1.300	1.193	0.773	0.935	0.627
4	1.120	0.997	0.725	0.846	0.506
5	1.446	1.380	1.082	1.262	0.357
6	1.043	1.020	0.718	0.675	0.559
7	0.767	0.771	0.826	0.924	0.321
8	0.943	1.443	0.774	0.870	0.408
9	0.449	0.429	0.296	0.345	0.228
10	0.527	0.573	0.277	0.410	0.301
11	0.737	1.003	0.355	0.396	0.345
12	0.663	0.903	0.319	0.356	0.311
13	1.693	1.731	1.001	1.070	0.917
14	1.863	1.740	0.785	0.974	0.379
15	0.696	0.906	0.507	0.439	0.775
16	0.626	0.815	0.456	0.395	0.698
17	0.693	0.820	0.525	0.647	0.453
18	1.863	1.740	0.785	0.974	0.379
19	0.573	0.762	0.868	0.744	0.633
20	1.043	1.020	0.718	0.675	0.559

transformation system. At the end of each member, the zero-length rotating springs are placed following the assumptions mentioned in the other members of Sections 1–3 to consider the effects of the presence of the gusset plate in the connection zones. Figure 11 provides a similar view of the modeling method in the present study for the execution details at the connection zone of the beam and the brace to the column.

Figure 12 also schematically shows the mathematical model of the arrangement of the springs for a braced bay of the frames.

In horizontal beams with hinges, according to Hsiao [25], in addition to end rotating springs, due to the simple system type in the bracing frames of the main beam element, the "Beam with hinge" element should be used and create a "pin" at both ends of the beams. Therefore, the buckling

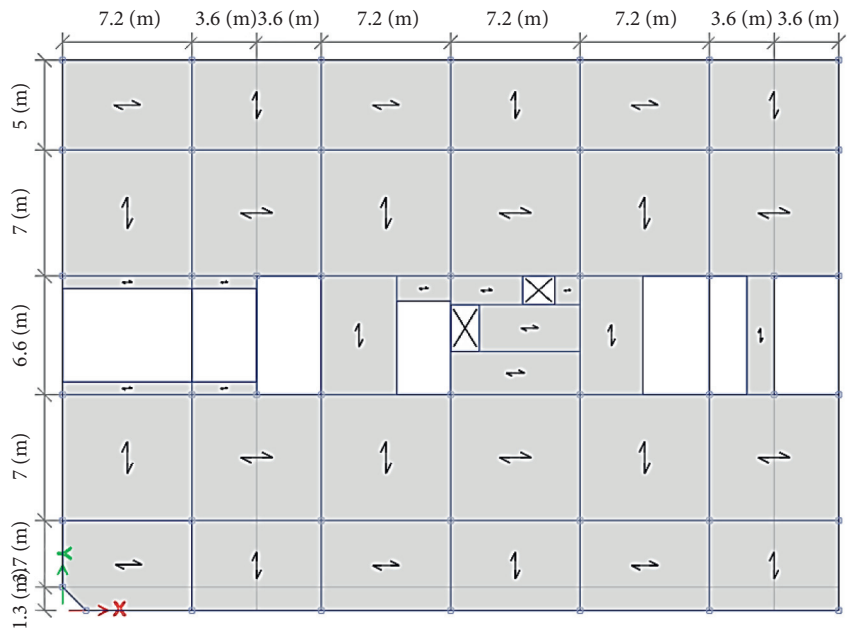

Figure 7: Plan of structures and load-bearing direction of floors.

Table 4: Naming the frames under study.

No	System	Number of floors	Symbol
1	Ordinary concentrically braced frame	5	OBF-5
2	Special concentrically braced frame	5	SBF-5
3	Special concentrically braced frame	10	SBF-10
4	Special eccentrically braced frame	5	EBF-5
5	Special eccentrically braced frame	10	EBF-10

Table 5: Specifications of steel and concrete materials used.

Steel material type ST-37	
Elasticity module, E	$2.1 * 10^7$ ton/m^3
Yield stress, F_y	24000 ton/m^2
Ult. strength, F_u	37000 ton/m^2
Weight per volume	7.85 ton/m^3
Concrete material type C-25	
Elasticity module, E	$2.5 * 10^6$ ton/m^3
Rebars yield stress, F_y	40000 ton/m^2
Transverse rebar yield stress, fys	37000 ton/m^2
Weight per volume	2.5 ton/m^3
Compressive strength	2800 ton/m^2

behavior of the braces can occur in or out of the plane. Concentric restraints are crosswise and with a connecting plate at the point of collision of the two restraints and the point of impact with the beams, the vertical and axial forces are not absorbed in the gusset plate. In this regard, the research of Astaneh-Asl et al. from the University of Michigan (1981 to 1986) showed that the cyclic behavior of brace sheets strongly depends on the buckling direction of the brace member. This means that when the bracing member buckles in-plane, three plastic hinges can form in the member, one in the middle of each member's length and one at each end of each member just outside the gusset plate. Therefore, the braces rotate at the hinge place. However, just after the gusset plate, we will have a detailed behavior due to the simplicity of the structural frame system. The brace behaves almost elastically in this type of buckling [26]. The mathematical model of the bracing frame can include the hinges at the end of the members. However, in reality, due to the connection of the gusset plate, we will not see the hinge behavior exactly at the connection. We see this exactly after the gusset plate.

3.3. Eccentric Bracing Frames

3.3.1. Frame Modeling with Eccentric Bracing. The conditions of the abutment and the arrangement of the restraints are modeled as structures with concentric restraints. The Standard 2800 for such frames only confirms remarkable ductility. Therefore, only 2 structural models have been made in such frames. The length of the beam is decided by the criteria of Article 10 of the National Building Regulations of Iran and Code 360 of the Iran Program and Budget Organization. Also, in this case, the Standard 2800 factor of performance related to the calculation of earthquake coefficient in these frames is considered one unit higher than other link beams, so in this study, to optimize sections due to seismic force reduction, the length of link beams is less than that. It is noteworthy that both the shear and flexural behavior of the beams are considered in modeling and analysis to pay attention to the responses. Figure 13 shows an overview of a 10-story frame model and a 3D model. Also, the sections obtained in the design by the criteria of Article 10 of the National Building Regulations of Iran and Standard 2800 for different members of Eccentric frames are listed in

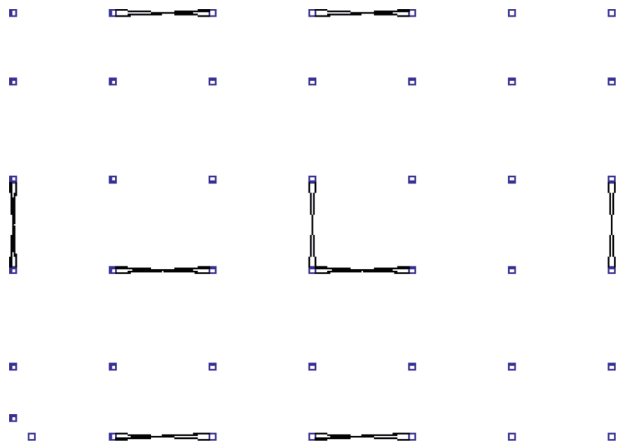

Figure 8: Arrangement of braces in the plan.

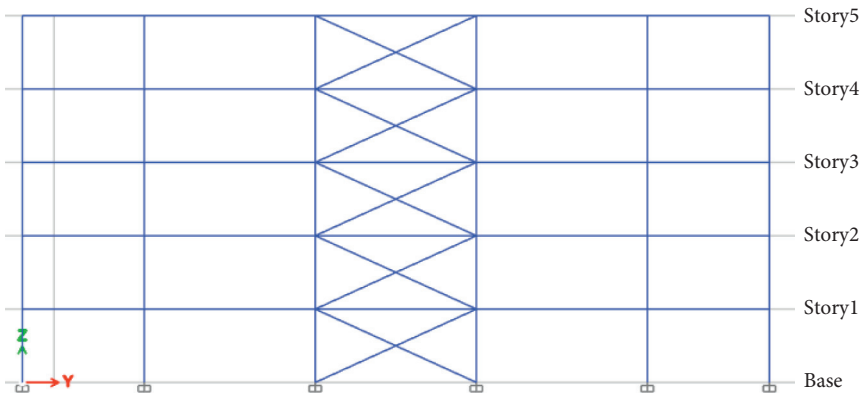

Figure 9: View of the selected two-dimensional frame.

Table 6: Sections obtained for different structural members in frames with concentric bracing.

Floor	Column	Beam	Brace
OBF-5			
1 to 5	BOX 450 ∗ 450 ∗ 20	IPE 330	TUBO 200 ∗ 200 ∗ 20
SBF-5			
1 to 5	BOX 450 ∗ 450 ∗ 30	IPE 330	TUBO 180 ∗ 180 ∗ 20
SBF-10			
1 to 5	BOX 450 ∗ 450 ∗ 25	IPE 450	TUBO 180 ∗ 180 ∗ 20
6 to 10	BOX 400 ∗ 400 ∗ 25	IPE 360	TUBO 180 ∗ 180 ∗ 20

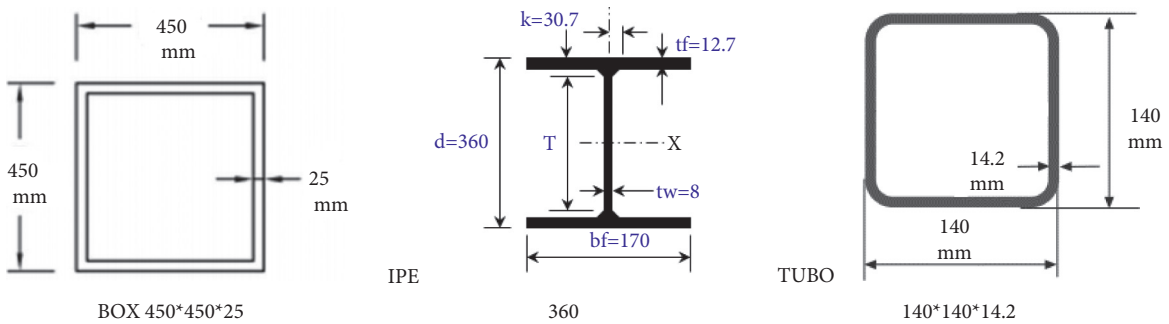

Figure 10: An example of each section type that used in concentric bracing frames.

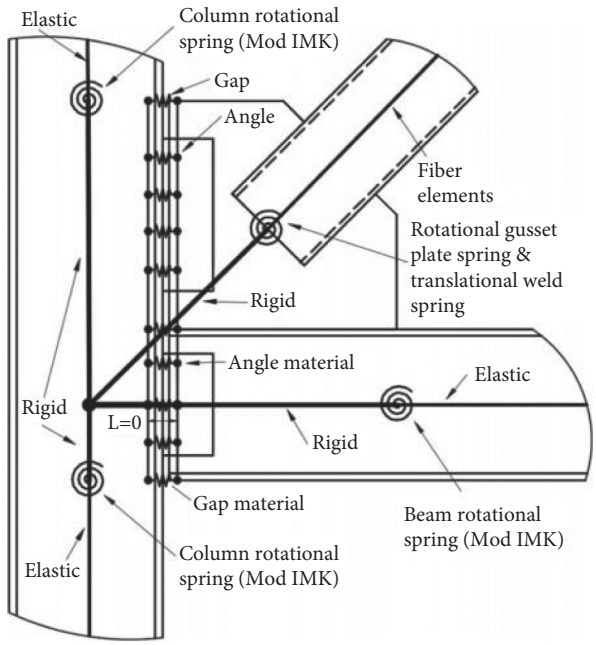

Figure 11: Numerical model schematic for connection zone of a braced frame beam-column [24].

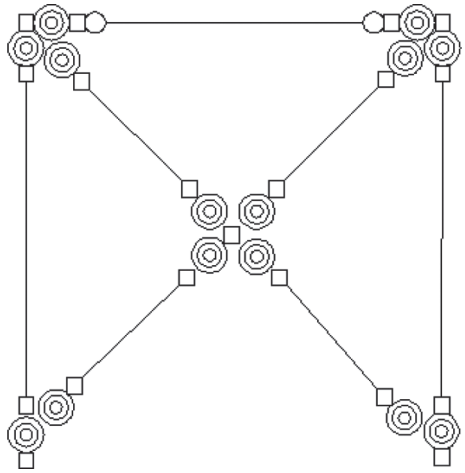

Figure 12: Mathematical model of a single bay concentric bracing frame.

Table 7, and for an example, the execution detail used for one of the link beams is shown schematically in Figure 14.

Main beams in these frames can have simple connections to the columns in cases where the link beam is located in the middle of the beam and away from the columns and connection zones [2]. Considering the mentioned effects, as mentioned by Hu et al., it is possible not to assume an interaction between shear and flexural behavior in the beam [27] because according to the classification in AISC360-16 and Code 360 of Iran, the behavior of link beams in modeled frames according to their length of 50 cm is in the category of shear behavior. It should be noted that according to Popov's research, $e = 1.6 * Mp/Vp$ is the boundary between shear and flexural behavior in these frames [3, 28]. According to Figure 15 with two rotating springs and two transfer zero-length springs at the end of the member, the mathematical model of the link beam simultaneously observes its shear behavior and flexural behavior.

According to Figure 16, modeling of other members according to their modeling in the frames of other structural systems of this research has been done with a concentrated plasticity approach.

3.3.2. Validation of Modeling Method. Shi et al. performed an experimental study on an eccentric bracing frame [29]. In this experiment, which is on a frame with geometric characteristics according to Figure 17, by pushing the frame, they drew a push curve according to Figure 18, which is used for modeling validation. In this experiment, they have for steel material $E = 210\,\text{kN/mm}^2$ and $Fy = 306\,\text{N/mm}^2$.

According to the experimental conditions, this frame was modeled in OpenSees and ETabs software. The push curve was drawn, which can be seen in Figure 19. In order to compare the results of the experiment by Shi et al. and the modeling performed according to the frames of this experiment, the ultimate force and displacement endured are collected (Table 8). The results show that the difference between the experimental results and the modeling in both software is less than 10%.

4. Analysis of Models

4.1. Incremental Dynamic Analysis of Frames. By selecting the first earthquake record and its first scale (one-tenth "g" (acceleration of gravity) higher in each step), the incremental dynamic analysis of the introduced frame begins to record the displacements of the frame at each story by the excitation pattern of its base and the maximum amount of interstory drift and its acceleration. The title of the representative point of this scale is recorded from each record and the frame response in other scales until the maximum class displacement reaches the mentioned limit in the drift criteria. The algorithm is repeated for each record, and IDA diagrams of each record can be drawn. The response of a structure under ground motion can be estimated with appropriate accuracy by performing a dynamic analysis of time history. One of the most important drawbacks of applying nonlinear dynamic analysis is the sensitivity of the response to selected accelerometers. The presentation of incremental dynamic analysis and estimation of responses based on the application of probabilistic relations have to a large extent be compensated for this weakness in practice. The results of IDA analysis obtained from this method along with 16,50,84% percentiles (the smaller percentiles in the chart are higher than the larger percentiles) and the probability density function (PDF) of the data are plotted in Figures 20–22, in addition to the points selected due to the reduction of stiffness to 20% of the elastic stiffness of each curve. Further examination is indicated in these curves.

4.2. Collapse Prevention Performance Level. Collapse prevention performance level refers to the performance level

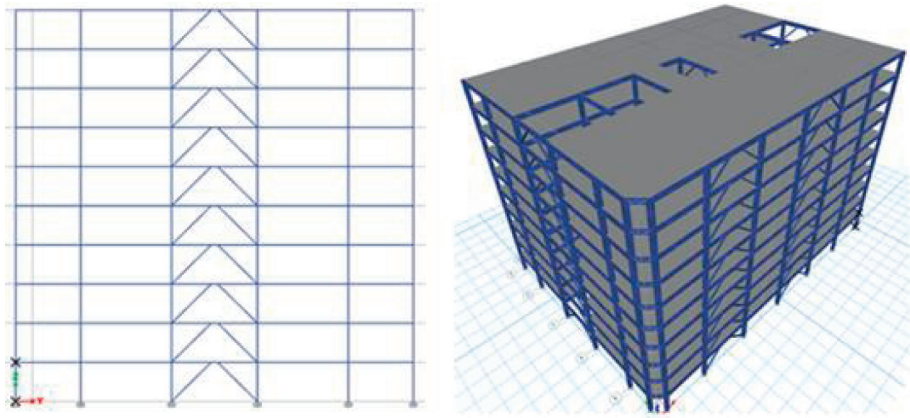

Figure 13: Overview of a simple structural frame model with an eccentric bracing system.

Table 7: Sections obtained for different structural members in frames with an eccentric bracing system.

Floor	Column	Beam	Brace	Link beam stiffner
EBF-5				
1 to 5	BOX 450 ∗ 450 ∗ 25	IPE 360	TUBO 140 ∗ 140 ∗ 14.2	7 ∗ 2PL 34 ∗ 9 ∗ 1
EBF-10				
1 to 5	BOX 450 ∗ 450 ∗ 25	IPE 500	TUBO 180 ∗ 180 ∗ 20	7 ∗ 2PL 47 ∗ 10 ∗ 1
6 to 10	BOX 400 ∗ 400 ∗ 25	IPE 450	TUBO 180 ∗ 180 ∗ 20	7 ∗ 2PL 42 ∗ 9 ∗ 1

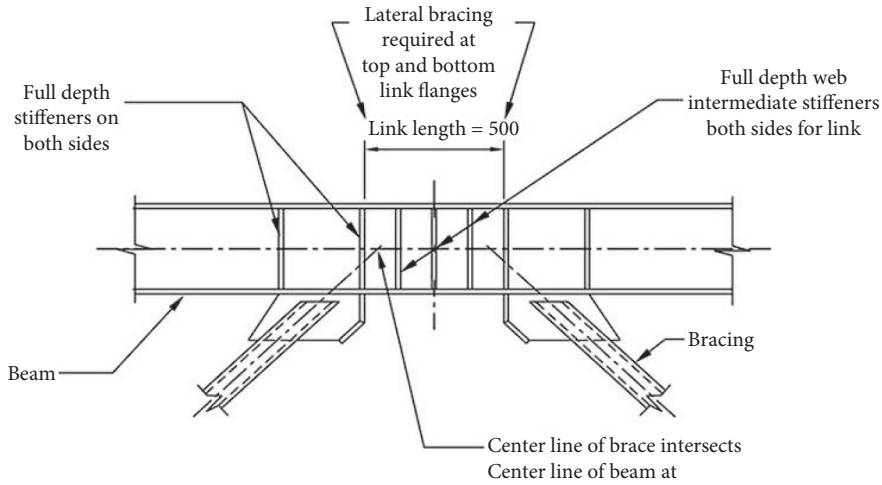

Figure 14: A schematic example of the execution detail used for one of the link beams.

Figure 15: Schematic model of link beams in eccentric frames.

predicted to cause extensive damage to the structure due to an earthquake. However, the structure collapses and lateral losses are minimized. In this case, there is a significant reduction in stiffness and strength of the lateral force system.

In this study, FEMA-356 indicates a drift limit of 5% for frames up to 8 floors and FEMA-273 for higher frames such as 10-story bracing frames. This drift ratio is acceptable up to 4% [30]. The model is performed to the extent that if static instability occurs in the structure with decreasing degrees of uncertainty, the collapse will be probable. In other cases, the hysteresis curve of the braces in tension and pressure according to their behavior due to the possibility of buckling in modeling according to what was mentioned in the relevant section will be the criterion for calculating the displacements [25]. In conclusion, in Table 9, the limits that have been used for the drift criterion in collapse for each system in fragility analysis and the functional level of

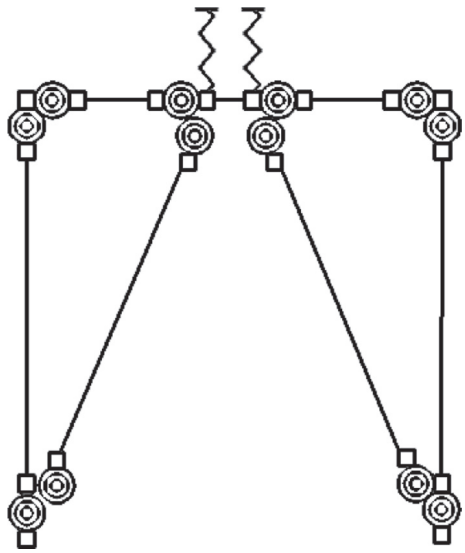

Figure 16: Analytical model of an eccentric bracing single bay frame.

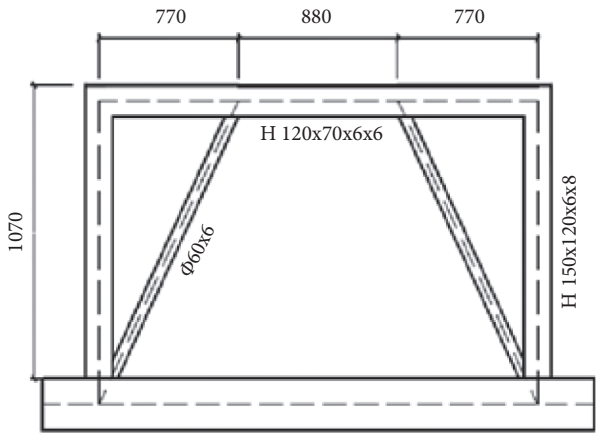

Figure 17: Geometric characteristics and sections used in the experiment by Shi et al. [29].

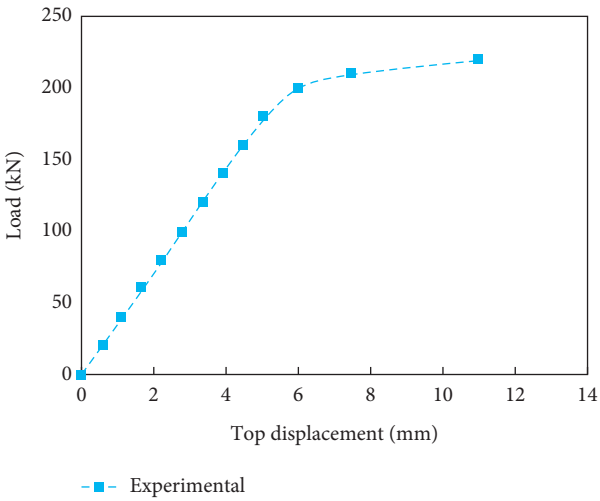

Figure 18: Frame push curve resulting from experiment [29].

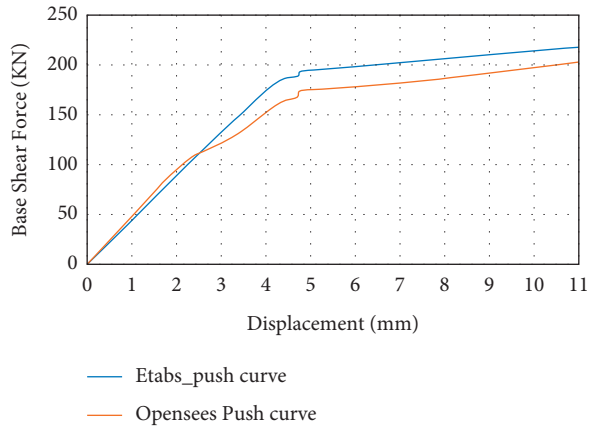

Figure 19: Results obtained from eccentric frame modeling in OpenSees and ETabs software.

collapse as the level considered for systems review in this research can be seen.

4.3. Uncertainties. To draw fragility curves and estimate the probability of collapse, we are faced with two main categories of uncertainty. Some of these uncertainties are inherent, and some are cognitive. For inherent uncertainties or record-to-record FEMA-P695, use the variance of the original data used to plot the fragility curves resulting from incremental dynamic analysis (spectral accelerations corresponding to the level of collapse threshold performance in each branch of the IDA curves in each frame) to consider this parameter. Cognitive uncertainties arise from differences in the definition of assumptions, ambiguous or unknown factors. FEMA-P695 identifies 3 parameters related to cognitive uncertainties (design, modeling, and test data) by qualitatively ranking their values. The designer must know in which category the assumptions are assumed to be excellent, good, average, or poor. In this research, the amount of 0.35 (average certainty) is assumed for these 3 parameters. Also, the final values of the uncertainty parameters, which is the 2nd root of the sum of the squares of all 4 uncertainties, are obtained for the studied models according to Table 10.

4.4. Achieving Fragility Curves. The fragility curve requires a change in the original variance of the data to be obtained from the combination of uncertainty parameters with "x" "μ" is an inversion of the natural logarithm of the middle of the data, "σ" is a variance of the data, and finally "Φ" is the Laplace integral. Using equation (5), new fragility curves can be obtained according to Figures 23–25 that gives the percent of probability of collapse against Sa (T1, 5%).

$$F(x) = \Phi\left(\frac{\ln x - \mu}{\sigma}\right). \quad (5)$$

4.5. Collapse Probability Analysis. In Sections 2 and 3, a uniform hazard spectrum was drawn for earthquakes with a

Table 8: Results of software modeling and validation by the experiment of Shi et al.

	Ultimate force (kN)	Ultimate displacement (mm)
Experiment (Shi et al.)	220	11
ETabs	219	11.32
OpenSees	207	11.92

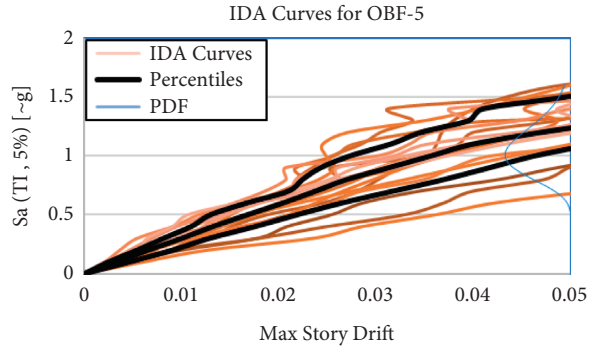

Figure 20: IDA curves obtained for OBF-5.

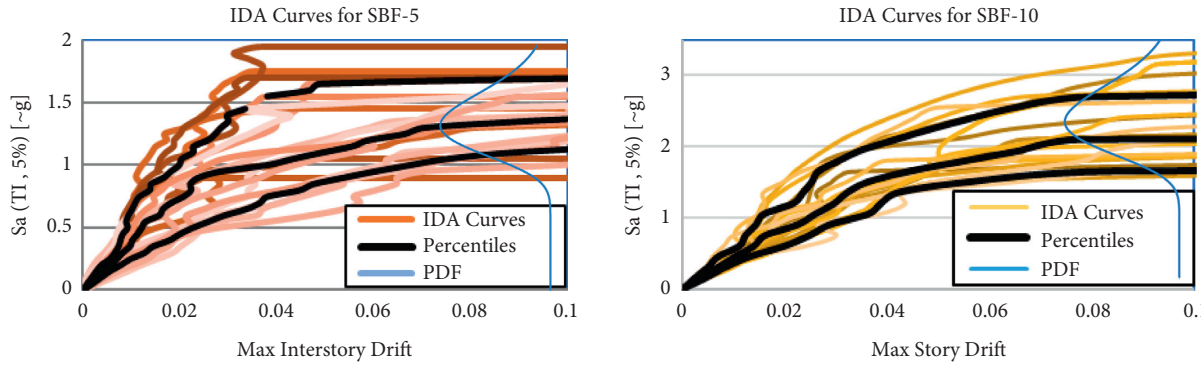

Figure 21: IDA curves obtained from right to left for SBF-10 and SBF-5, respectively.

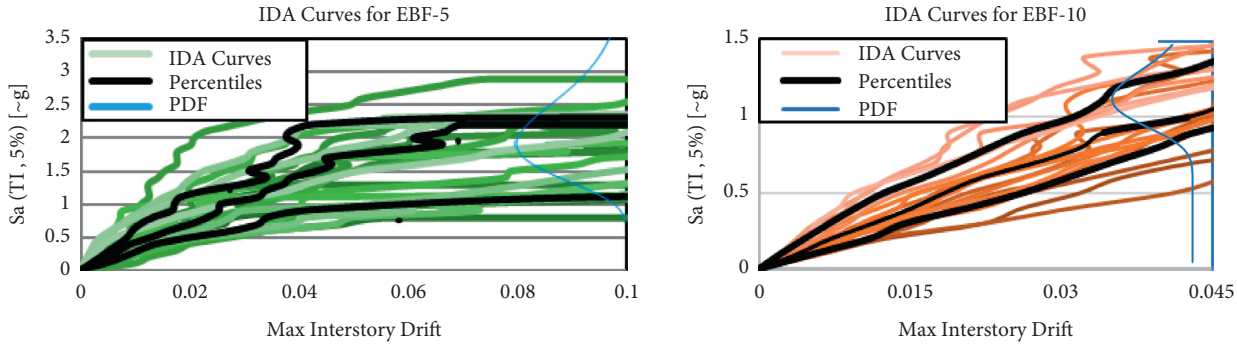

Figure 22: IDA curves obtained from right to left for EBF-5 and EBF-10.

return period of 2475 years. Based on this spectrum and the periodicity obtained for dynamic models of frames in OpenSees software, the amount of spectral acceleration can be taken from the mentioned hazard spectrum. This spectral acceleration uses fragility curves drawn for each model. The probability of their collapse can be deduced. In Table 11, the probabilities of the collapse of the studied models are obtained for the maximum ground motions.

In Table 11, once with only fragility curves in terms of record-to-record uncertainty and once with all uncertainties, the probability of collapse is obtained; in this study, the probabilities of collapse are obtained in the case of more

Table 9: Drift limit of collapse prevention for various structural systems.

No.	Frame	Limit	Ref.
1	OBF-5	0.05	FEMA-356
2	SCBF-5	0.05	FEMA-356
3	EBF-5	0.05	FEMA-356
4	SCBF-10	0.04	FEMA-273
5	EBF-10	0.04	FEMA-273

Table 10: Uncertainty parameters and their combination results.

Frame	Mean	Record to record	Design	Modeling	Test data	Total
OBF-5	0.53	0.21	0.35	0.35	0.35	0.64
SCBF-5	0.33	0.19	0.35	0.35	0.35	0.64
EBF-5	0.58	0.32	0.35	0.35	0.35	0.69
SCBF-10	0.85	0.22	0.35	0.35	0.35	0.64
EBF-10	0.56	0.17	0.35	0.35	0.35	0.63

uncertainty. We have, in all cases, been more in terms of uncertainty due to changes in fragility curves in the acceleration of the spectra. In addition, the acceptable limit for this type of analysis is the probability of total collapse of structures of similar importance to residential buildings is 10% (Table 11); the results show a deviation from this acceptable limit in the SBF-5 and OBF-5, which can be a warning for the design regulations of steel structures in the field of such structures. This is because in the design of structural models of this study, all the necessary controls in National Building Regulations of Iran and Standard 2800 have been observed.

5-story models with concentric bracing, whether extraordinary or ordinary ductility, as previously mentioned, could not be within the acceptable range in terms of the probability of collapse in both systems; in addition, for the fragility curves of EBF systems, the surface under the chart is higher, the periodicities of concentric bracing frames are generally shorter, and due to the uniform hazard spectrum, they have highest spectral acceleration, which makes it a higher probability of collapse for concentric bracing frames. So we can sometimes see that such designed structures with conventional codes are not within acceptable limits. It is also observed between different structural systems that if a more ductile type is used (for example, a particular concentric bracing frame instead of an ordinary concentric bracing frame), the probability of collapse will decrease.

Comparing the designed 10-story models, the results show that for 10-story frames, special concentric bracing and eccentric bracing have acceptable seismic safety. Even the acceptable range shows that one of the essential points in choosing a structural system is to pay attention to their performance due to changes in mass and stiffness due to changes in height and number of floors. It can also be said that special concentric bracing frames and unique eccentric bracing frames in the 10-story elevation system are safe against collapse. Table 12 shows the probability of collapse

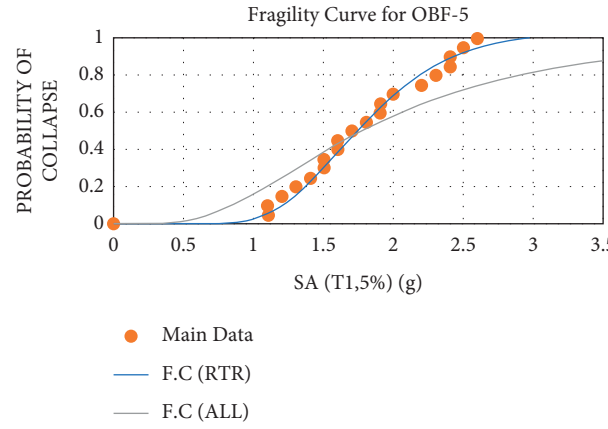

Figure 23: Fragility curves of OBF-5 frame with all uncertainties.

for significant buildings such as hospitals and national museums.

5. Summary and Conclusion

In this research, 5 steel is used for structural frames in different structural systems heights such as simple construction frames. These frames were then evaluated for probabilities at the performance level of collapse prevention. The results obtained, although not used in general to all structures, but in the field of this research include the following:

(i) Considering that the frames studied in this research are designed based on the codes of National Building Regulations and Standard 2800, which are the common structure design regulations in Iran, and considering that 2 frames with bracing including SBF-5 and OBF-5, the probability of collapse was higher than acceptable. That means these codes need revision.

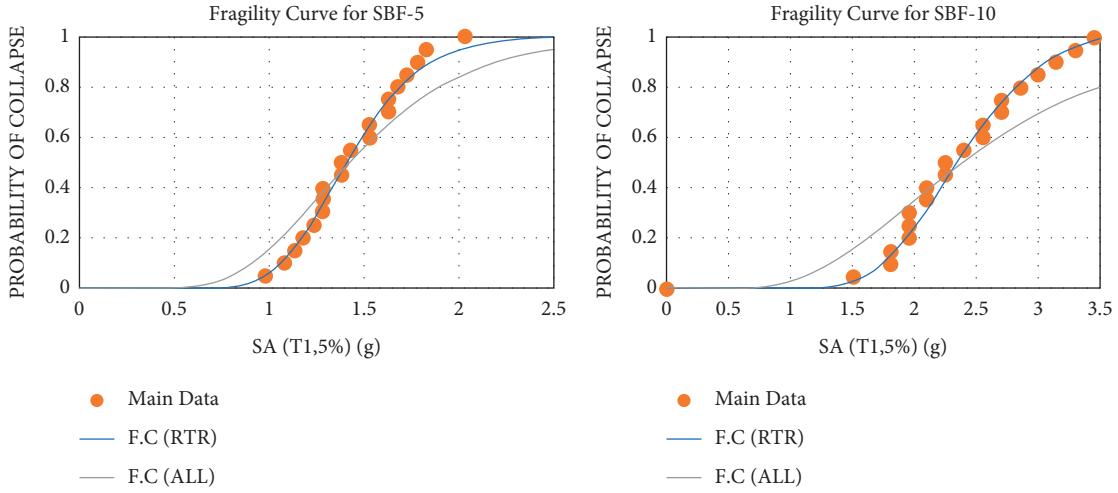

Figure 24: Fragility curves of SBF-5 and SBF-10 frames with all uncertainties.

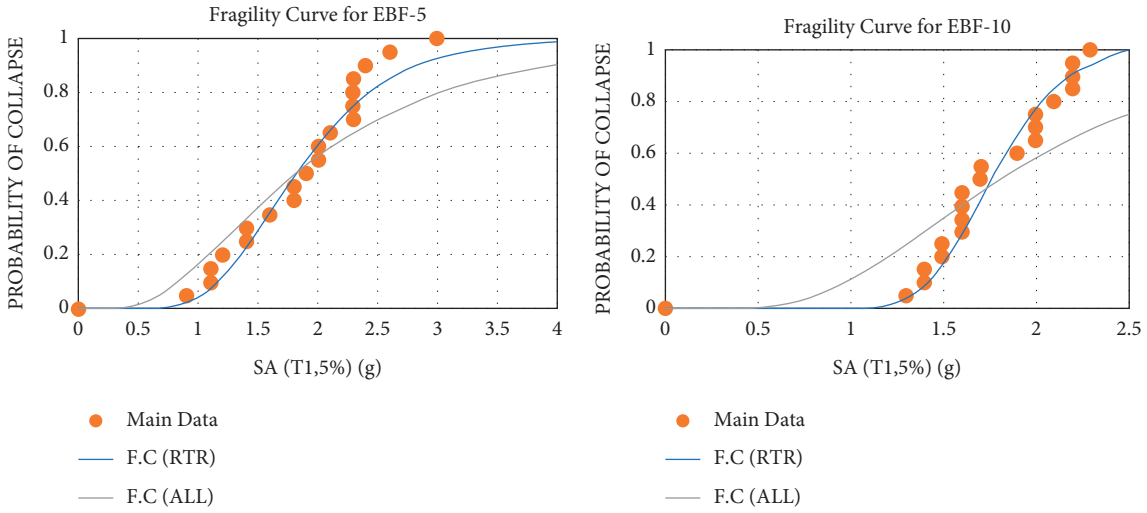

Figure 25: Fragility curves of EBF-5 and EBF-10 frames with all uncertainties.

Table 11: Probability of collapse of structural frames.

Frame	Spectrum		Collapse probability	
	Period (s)	Acceleration	RTR	ALL
SBF-5	0.587	1.07	0.04	0.14
SBF-10	0.848	0.74	0.0001	0.01
OBF-5	0.65	0.97	0.02	0.15
EBF-5	0.842	0.75	0.005	0.07
EBF-10	1.179	0.53	0.003	0.015

Table 12: Probability of collapse for important members in structural stability and noncritical members [13].

Target reliability (conditional probability of failure) by the MCE$_r$ shaking hazard (%)		
Risk category	For structural stability	For noncritical members
I, II	10	25
III	5	15
IV	2.5	9

(ii) Increasing ductility in systems (such as using unique frames instead of ordinary frames) could reduce the probability of collapse.

(iii) One of the essential points in choosing a structural system is to pay attention to their performance due to changes in mass and stiffness due to changes in height or number of floors. For example, among 5-story frames, only the EBF-5 frame is within the acceptable

probability of collapse. However, in 10-story frames, both the SBF system and the EBF system were able to have an acceptable probability of collapse. For 10-story frames, the probability of collapse in both systems can be used instead of residential use for more important use, such as hospitals.

Data Availability

The data used to support the findings of this study are included within the article.

Conflicts of Interest

The authors declare no conflicts of interest.

References

[1] I. Mhud, *National Building Code, Part 10, Steel Structure Design*, Ministry of Housing and Urban Development, Tehran, Iran, 2009.

[2] F. Naeim, *The Seismic Design Handbook*, Springer Science & Business Media, Springer, Berlin, 1989.

[3] E. P. Popov and M. D. Engelhardt, "Seismic eccentrically braced frames," *Journal of Constructional Steel Research*, vol. 10, pp. 321–354, 1988.

[4] S. D. Hague, "Eccentrically braced steel frames as a seismic force resisting system," Master's thesis, Kansas State University, Manhattan, KN, USA, 2013.

[5] N. Ghorbani and A. Korzeniowski, "Adaptive risk hedging for call options under cox-ingersoll-ross interest rates," *Journal of Mathematical Finance*, vol. 10, no. 4, pp. 697–704, 2020.

[6] Q. Shi, S. Yan, X. Wang, H. Sun, and Y. Zhao, "Seismic behavior of the removable links in eccentrically braced frames with semirigid connections," *Advances in Civil Engineering*, vol. 2020, Article ID 9405107, 26 pages, 2020.

[7] G. G. Deierlein and C. B. Haselton, "Developing consensus provisions to evaluate collapse of reinforced concrete buildings," in *Proceedings of the US-Japan DaiDaiToku/NEES Workshop on Seismic Response of Reinforced Concrete Structures*, pp. 7-8, Tokyo, Japan, 2005.

[8] J. Yaser Mozaffari and N. Abbas Akbarpour, "Assessing behavior of structural due to near-field earthquake," *International Journal of Civil Engineering and Building Materials*, vol. 2, no. 2, 2012.

[9] A. Bakhshi and H. Soltanieh, "Development of fragility curves for existing residential steel buildings with concentrically braced frames," *Scientia Iranica*, vol. 26, no. 4, pp. 2212–2228, 2019.

[10] T. Y. Yang, H. Sheikh, and L. Tobber, "Influence of the brace configurations on the seismic performance of steel concentrically braced frames," *Frontiers in Built Environment*, vol. 5, p. 27, 2019.

[11] D. Vamvatsikos and M. Fragiadakis, "Incremental dynamic analysis for estimating seismic performance sensitivity and uncertainty," *Earthquake Engineering & Structural Dynamics*, vol. 39, no. 2, pp. 141–163, 2010.

[12] K.-C. Lin, C.-C. J. Lin, J.-Y. Chen, and H.-Y. Chang, "Seismic reliability of steel framed buildings," *Structural Safety*, vol. 32, no. 3, pp. 174–182, 2010, þ.

[13] Asce 7-10, *Minimum Design Loads for Buildings and Other Structures*, American Society of Civil Engineering (ASCE), Reston, VA, USA, 2010.

[14] N. Shome, *Probabilistic seismic demand analysis of nonlinear structures*, Stanford University, Phd thesis, 1999.

[15] D. Vamvatsikos and C. Allin Cornell, *Seismic performance, capacity and reliability of structures as seen through incremental dynamic analysis*, Stanford University, Phd thesis, 2002.

[16] Y. Bozorgnia, M. Rahnama, and M. Berberian, "Probabilistic seismic hazard analysis, phase I–greater Tehran regions," Final report, Faculty of Engineering, University of Tehran, Tehran, Iran, 2008.

[17] A. Azarbakht and M. Dolšek, "Progressive incremental dynamic analysis for first-mode dominated structures," *Journal of Structural Engineering*, vol. 137, no. 3, pp. 445–455, 2011.

[18] X. Zhao, W. D. Zhu, and Y. H. Li, "Analytical solutions of nonlocal coupled thermoelastic forced vibrations of micro-/nano-beams by means of green's functions," *Journal of Sound and Vibration*, vol. 481, Article ID 115407, 2020.

[19] Federal Emergency Management Agency, "Engineering guideline for incremental seismic rehabilitation," Report No. FEMA-P420, Federal Emergency Management Agency, Washington, DC, USA, 2009.

[20] H. Krawinkler, F. Zareian, D. G. Lignos, and L. F. Ibarra, "Prediction of collapse of structures under earthquake excitations," in *Proceedings of the 2nd International Conference on Computational Methods in Structural Dynamics and Earthquake Engineering*, pp. 22–24, Rhodes, Greece, June 2009.

[21] H. Huang, M. Huang, W. Zhang, and S. Yang, "Experimental study of predamaged columns strengthened by HPFL and BSP under combined load cases," *Structure and infrastructure engineering*, vol. 17, no. 9, pp. 1210–1227, 2020.

[22] D. G. Lignos and H. Krawinkler, "Sidesway collapse of deteriorating structural systems under seismic excitations," Rep. No. TB 172, John A. Blume Earthquake Engineering Center, Stanford, CA, USA, 2009.

[23] P. Uriz and S. Mahin, "Toward earthquake resistant design of concentrically braced steel frame structures," PEER Report 2008/08, University of California, Oakland, CA, USA, 2008.

[24] J. Sizemore, *Inelastic behavior and seismic collapse prevention performance of low-ductility steel braced frames*, Ph.D. dissertation, Dept. of Civil and Environmental Engineering, Univ. of Illinois at Urbana-Champaign, Urbana-Champaign, IL, USA, 2017.

[25] P.-C. Hsiao, *Seismic performance evaluation of concentrically braced frames*, University of Washington, Seattle, WA, USA, PhD diss, 2012.

[26] A. Astaneh-Asl, S. C. Goel, and R. D. Hanson, "Cyclic out-of-plane buckling of double-angle bracing," *Journal of Structural Engineering*, vol. 111, pp. 1135–1153, 1985, þ.

[27] S. Hu, Z. Wang, and Z. Wang, "Practical advanced analysis for eccentrically braced frames," *Advanced Steel Construction*, vol. 11, no. 1, pp. 95–110, 2015.

[28] Z. Alam, L. Sun, C. Zhang, Z. Su, and B. Samali, "Experimental and numerical investigation on the complex behaviour of the localised seismic response in a multi-storey plan-asymmetric structure," *Structure and infrastructure engineering*, vol. 17, no. 1, pp. 86–102, 2020.

[29] Y. J. Shi, J. Xiong, Y. Q. Wang, and G. Liu, "Experimental studies on seismic performance of multi-storey steel frame with eccentric brace," *Journal of Building Structures*, vol. 31, no. 2, pp. 29–34, 2010.

[30] Federal Emergency Management Agency, "NEHRP guidelines for the seismic rehabilitation of buildings," Report No. FEMA-273,, Federal Emergency Management Agency, Washington, DC, USA, 1997.